J Neurophysiol 115: 2519–2528, 2016.
First published March 2, 2016; doi:10.1152/jn.00043.2016.

The predictive roles of neural oscillations in speech motor adaptability

Ranit Sengupta and Sazzad M. Nasir
Department of Communication Sciences and Disorders, Northwestern University, Evanston, Illinois

Submitted 14 January 2016; accepted in final form 25 February 2016

Sengupta R, Nasir SM. The predictive roles of neural oscillations in speech motor adaptability. *J Neurophysiol* 115: 2519–2528, 2016. First published March 2, 2016; doi:10.1152/jn.00043.2016.—The human speech system exhibits a remarkable flexibility by adapting to alterations in speaking environments. While it is believed that speech motor adaptation under altered sensory feedback involves rapid reorganization of speech motor networks, the mechanisms by which different brain regions communicate and coordinate their activity to mediate adaptation remain unknown, and explanations of outcome differences in adaption remain largely elusive. In this study, under the paradigm of altered auditory feedback with continuous EEG recordings, the differential roles of oscillatory neural processes in motor speech adaptability were investigated. The predictive capacities of different EEG frequency bands were assessed, and it was found that theta-, beta-, and gamma-band activities during speech planning and production contained significant and reliable information about motor speech adaptability. It was further observed that these bands do not work independently but interact with each other suggesting an underlying brain network operating across hierarchically organized frequency bands to support motor speech adaptation. These results provide novel insights into both learning and disorders of speech using time frequency analysis of neural oscillations.

EEG; motor speech adaptation; neuronal oscillations

ONE OF THE HALLMARKS OF THE human speech production system is its ability to adapt under a variety of distortions in speech environments (Houde and Jordan 1998; Jones and Munhall 2005; Purcell and Munhall 2006; Tremblay et al. 2003; Villacorta et al. 2007; Nasir and Ostry 2006; Lametti et al. 2012). This adaptive ability is a fundamental trait of the brain and is critical for normal speech development and language learning abilities (Perkell 2012; Guenther 2006), and its breakdown can cause debilitating speech disorders such as stuttering (Cai et al. 2012) and ataxia (Zeigler and Wessel 1996). Speech motor adaptation, unlike motor learning in human arm movement tasks, exhibits a wide range of individual differences across subjects. In studies of motor speech adaptation under altered sensory feedback, both for auditory and somatosensory perturbation, differences in individual responses have been noted wherein some subjects who do not adapt under altered auditory feedback may adapt under somatosensory feedback and vice versa, while others do not adapt to the task at all (Lametti et al. 2012). Since very little is known about the neural basis of speech motor learning, a careful and systematic study of outcome differences will elucidate the factors, processes, and brain regions that contribute to such variability in motor speech adaptation.

The present study aims to investigate this question of outcome differences in adaptation by examining oscillatory brain activity in EEG recordings while subjects perform a speech motor training task under altered auditory feedback. In particular, the study tests the idea that adaptation differences are captured and predicted by distinctive EEG spectral profiles and, therefore, elucidates the differential role of the various EEG frequency bands in motor speech adaptation. EEG frequency bands have been found to play specific roles in different aspects of motor control (Lisman and Jensen 2013; van Wijk et al. 2012), with distinct bands contributing to planning, executing, and feedback control. For example, the gamma band plays a role in voluntary motor control (Douglas et al. 2008; Cheyne et. al. 2008), beta band plays a role in motor planning (McFarland et. al. 2000; Tzagarakis et. al. 2010), and theta-band activity modulates higher frequency beta and gamma bands during both planning and execution of motor tasks (Canolty et. al. 2006; Perfetti et. al. 2011) and alpha band in sensory perception (Strauss et al. 2014). More recently, neural oscillations have also been implicated in the context of human speech (Arnal and Giraud 2012; Arnal et al. 2011; Giraud and Poeppel 2012; Sengupta and Nasir 2015). We therefore expect these frequency bands to be involved in motor speech adaptability.

This paper aims to address the involvement of neural oscillations at the scalp electrode level in two steps: first, what are the electrodes and the frequency band activities at them that correlate with the degree of speech motor adaptation, and second, how much reliable information is contained in these activities based on which one can predict whether subjects will adapt or not. Our analyses revealed that only a handful of electrodes contained reliable information in the low-frequency theta band, medium-frequency beta band, and high-frequency gamma band based on which accurate prediction on adaptation outcome was possible. Moreover, it was found that the bands do not operate independently but interact with one another demonstrating how coupled frequency bands support adaptive behavior through brain networks operating across multiple spatiotemporal scales. Such a predictive analysis (Waldert et al. 2008; Markser et al. 2015; Wang et al. 2010; Quandt et al. 2012; Freyer et al. 2013; Brodski et al. 2015; Myers et al. 2014) will not only illuminate the mechanisms underlying the development of speech learning but will also aid in our understanding the basis of speech motor disorders.

METHODS

Subjects

Study participants included 17 male subjects between the ages of 19 and 30 (21.7 ± 0.6 yr). All subjects were English speakers without any known history of hearing or speech disorders. The Northwestern University Research Ethics Board approved all experimental procedures, and informed consent was obtained from all subjects before their participation in this study.

Address for reprint requests and other correspondence: S. M. Nasir, Dept. of Communication Sciences and Disorders, Northwestern Univ. 2240 Campus Dr., Evanston, IL 60208 (e-mail: s-nasir@northwestern.edu).

Experimental Setup and Task

Experiments were conducted in a soundproof booth. The experimental task consisted of speech motor training under continuous recording of EEG. A target word "Head" was displayed on a computer monitor and the subjects were instructed to read aloud the word as it appeared on the screen. Each subject repeated the target utterance for 8 baseline blocks followed by 12 training blocks and 5 after-effect blocks. Each block consisted of 12 trials each. Our goal was to investigate the mechanisms of adaptation, and hence, the analyses focused on the baseline and training phases only. Moreover, the after-effect persisted much longer without reaching the baseline level and was excluded from further analyses. A pause of 1–2 min between blocks and 2.5 s between trials was inserted to prevent fatigue. Subjects received normal auditory feedback in the baseline and after-effect phases, while in the training phase auditory feedback was perturbed by shifting the first two formant frequencies of the target vowel /æ/ towards /I/ as in "Hid" (Fig. 1*A*). Estimates of formant shifts were obtained at the start of the experiment for each subject during a screening phase when the vowel space was mapped out. The intensity of the feedback signal played back to participants was adjusted to 80 dB to minimize air-borne unaltered auditory feedback. A masking noise of 60 dB was also delivered through the headphones to minimize any bone-conducted unaltered feedback.

Neural activity was assessed during the baseline and at early and late training phases (defined below; also see Sengupta and Nasir 2015). A time window extending from 300 ms before to 600 ms after the voice onset was selected for analyzing the data so as to capture the neural processes related to speech planning (300 ms before voice onset), production (300 ms after the onset), and feedback error processing (300 ms following production) within each utterance.

Altered Feedback

The formant frequencies of the vowels were altered in real time during speech production following the methods of altered auditory feedback paradigm (Jones and Munhall 2005; Purcell and Munhall 2006). The LabView real time language implemented in the National Instruments PXI system can estimate the formant frequencies using the Burg algorithm and update the linear predictive coding (LPC) filter coefficients of the speech signal at a rate of 10 kHz. The participant's voice was recorded at 10 kHz to obtain offline estimates of the formant frequencies.

Acoustical Analyses and Learning

PRAAT and customized Matlab routines were used to extract the first and second formant frequencies of each utterance of the target sound for each subject. The formant frequencies were normalized by subtracting their baseline mean. To assess speech motor adaptation, the focus was only on the produced first formant frequency (f1) as the shifts in the second formant frequency (f2) were much less (~10% of the f2 value of head) compared with shifts in f1 (~25%) (Fig. 1*B*). Formant compensation was measured over the course of training and assessed for statistical significance (see below) between the early and late training phases at $P < 0.01$. A regression line was fitted over all the training trials and the slope was used as an estimate for the degree of adaptation; a significant positive slope implied successful adaptation while a negative slope implied nonadaptation. By this measure nine subjects adapted, called adapters, and eight did not and were termed nonadapters. It should be noted that there was no significant difference between the produced second formant frequencies of the two groups. An earlier paper (Sengupta and Nasir 2015) focused only on the adapters for investigating the role of theta-gamma phase coupling in the formation of feedforward map associated with adaptation. In the current study, we considered both adapters and non-

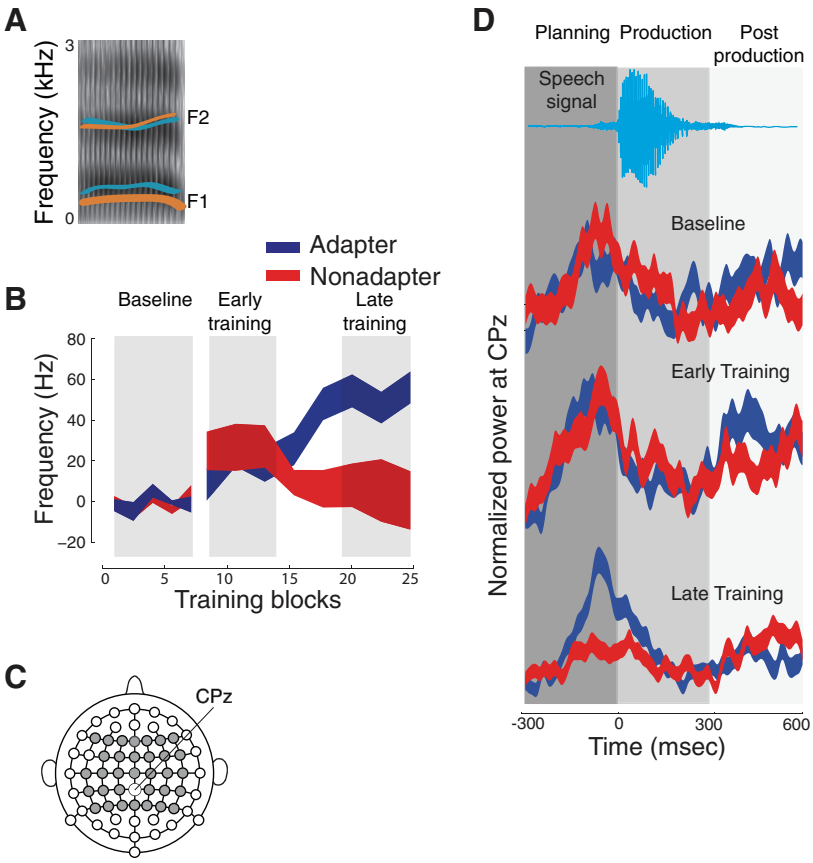

Fig. 1. Experimental setup. *A*: shifts in the first formant frequency during the utterance "Head." Blue trace shows the unperturbed 1st and 2nd formant frequency; red trace shows shifted formant frequency. *B*: averaged first formant frequency over the course of the experiment for adapters (blue) and nonadapters (red). Clear differences can be seen between two groups. Different experimental phase, baseline, early training and late training, are shown in grey. *C*: EEG signals were recorded from 26 electrodes spanning central, parietal, frontal and temporal scalp locations. *D*: overall power extracted at a representative electrode location, CPz, and averaged over the adapters and the nonadapters for different experimental phases. Differences between the two groups can be clearly seen in the total power between adapters, most conspicuously in late training. Also, note how the total power varies between adapters and nonadapters at different speech epochs. The line thickness indicates the standard error of mean.

adapters and examined the predictable roles played by the EEG frequency bands in accounting for outcome differences in speech motor adaptation. Neural activity was assessed during baseline and at early and late training phases. The baseline phase consisted of the last 50% of the trials in baseline, the early training phase consisted of the first 30% of the trials of the training phase, and the late training phase consisted of the last 30% of the trials of the training phase so that each of the phases contained equal number of trials.

EEG Acquisition

A 64-channel active Brainvision system was used to obtain EEG data at a sampling rate of 512 Hz using. The electrodes were mounted on an elastic cap following the standard 10–20 system of electrode placement and electrical impedances of the scalp electrodes were kept below 10 kΩ. For our analyses, we excluded electrodes over the occipital region and focused only on the electrodes on the temporal, parietal, and frontal areas of the scalp that are directly above the cortical regions supporting the speech motor task. We also excluded electrodes over the extreme temporal and frontal region to minimize movement artifacts and analyzed the remaining 38 electrodes indicated by gray circles in Fig. 1*C*. Participants were instructed to minimize eye blinks and head movements during word production and a brief hiatus between trials and blocks was inserted to prevent fatigue and muscle tension.

A TTL pulse delivered by the real-time Labview system was used for detecting of voice onset (Fig. 1*E*) and provided a time stamp for the alignment of the EEG signal and allowed for offline extraction of event-related potentials (ERPs).

Analysis of Power Orofiles

Filtering. The EEG signals were extracted using Matlab based EEGLAB toolbox. A second-order Butterworth filter was used to filter the signal offline between 0.75 and 55 Hz. The trial ERP epochs were then time aligned at the initiation of voice onset and extended from 900 ms before and after voice onset and re-referenced at electrode AFz. The average of the prevoicing part of the signal was subtracted before conducting further analyses.

Artifact rejection. Eye movements, head movement, and muscular activity giving rise to stereotypical artifacts arising were removed by detecting epochs in which the scalp voltage at any of the electrode locations exceeded 50 μV and excluding them from further analysis. Further artifact rejection was done to detect for the presence of aberrant temporal patterns, large negative kurtosis spectral peaks that coincided with muscle activation based on independent component analysis (Olbrich et al. 2011). The average number of trials discarded per subject was ~15%.

EEG frequency bands. The ERPs obtained were filtered to obtain the instantaneous power of rhythmic activity over five frequency bands: delta (1–3 Hz), theta (3–8 Hz), alpha (8–14 Hz), beta (14–30 Hz), and gamma (30–50 Hz). Each trial epoch was filtered using a fourth-order Butterworth filter to obtain the oscillatory component in each band. We then used the Hilbert transformation to obtain the instantaneous amplitude of the signal and squared it to obtain the power. Normalized power for each trial was obtained by dividing out by the overall power.

Generalized linear model analysis. To determine the electrode locations associated with speech motor adaptation, we first used a generalized linear model (GLM) (McCullagh and Nelder 1989) to quantify how the activity of the EEG power in each frequency band varied with the outcome of speech motor adaptation, as measured by the regression slope (see above). For each band, the instantaneous power levels averaged over a 10-ms time window slided in steps of 4 ms within the band was modeled as a linear weighted sum of the degree of adaptation. The average power within the window was calculated for each subject and then the power data and slopes for all 17 subjects were fed into the GLM model to obtain the linear weights. These weights capture the differences of the adaptation outcomes on power of the EEG frequency bands. We only chose those weights that were significant at $P < 0.01$ (uncorrected). The GLM analysis was carried out for each electrode location and at each frequency band separately to identify the electrodes within each band that accounted for the observed outcome differences. The coefficient obtained from the GLM was normalized between −1 and 1 before displaying on a scalp plot. A positive coefficient implies a positive relationship between power levels and adaptation outcome and vice versa.

Linear classification. To further examine the roles played by the EEG frequency bands in predicting behavioral outcome, a linear time-frequency pattern classification (Waldert et al. 2008) was carried out using the Matlab. For each subject, electrode location and frequency band the averaged power computed over 20-ms sliding window and in step of 4 ms were used for the classification analysis (Friedman et al. 2009). Each subject belonged to a single class of either an adapter or a nonadapter. With the use of these data, the classifier was trained on about half of the subjects and tested on the remaining half. This process was iterated for 4,000 times so as to obtain a large number of bootstrapped samples for carrying out the classification analyses. In each iteration the bootstrap sampling method without replacement (Efron 1982; Perfetti et al. 2011) was used to randomly select 9 subjects from a total of 17 that were used for training the classifier, while the remaining 8 subjects for testing the classifier. Partitioning of the training and test sets containing roughly equal number of subjects makes the classification task much harder and allows to obtain better estimate for classification accuracy. The statistical significance for classification was computed using Binomial distribution. The probability of success in correctly classifying an adapter or a nonadapter is 0.5 and achieving a success rate greater than 80% (at least 6 success out of 8) has a probability of $P < 0.03$. The average accuracy rate over all 4,000 bootstrap samples was then calculated and the electrode locations and the times for which the averaged accuracy crossed the threshold of 80% were determined. We thus obtained a set of electrodes within each frequency band and times that reliably predicted behavioral outcomes with an accuracy of 80% or better.

To evaluate the robustness of the bootstrapping procedure we calculated effect sizes associated with the classification accuracy rate. At the threshold crossings where the mean accuracy exceeds 0.5 (classification at the chance level), the effect sizes were at least 2.2 or greater with $P < 10^{-8}$.

Principal component analyses. Principal component (PC) analyses were performed to reveal cross-band interactions at the source level (Friedman et al. 2009). Separate PCs were computed for each frequency band by taking the data set from all 17 subjects. Analyses were conducted subsequently on the first three PCs as they account for up to 80% of the variance in the data. The above linear classification was conducted to identify the PCs contributing to outcome differences. To quantify cross-band interactions, covariance was computed between the PC time series across the frequency bands that crossed the classification threshold and the averaged covariance between adapters and nonadapters was compared using a *t*-test for statistical significance.

Statistical analysis. Adaptation for each subject was assessed using one-way ANOVA followed by Tukey's honestly significant difference to confirm that the adapted subjects altered their production significantly higher at the end of training relative to the baseline ($P < 0.01$).

Statistical significance of classification analyses was also conducted under the *t*-test and, separately, using repeated-measures two-way ANOVA. The analyses were carried out at each electrode location and using the same time windows as in the classification analyses. For ANOVA, statistical significance was ascertained when there was a main effect ($P < 0.05$) for the groups followed by Tukey's honestly significant difference ($P < 0.05$) that compared differences

between the adapters and nonadapters at early and late training phases. It should be noted that classification methods and ANOVA tap into different types of information and may not yield identical results.

RESULT

The goal of this study was to elucidate the role of the various EEG frequency bands in predicting behavioral outcomes of speech motor adaptation under the paradigm of altered auditory feedback. Subjects were asked to repeat the word "Head" under continuous recording of EEG. The experiment consisted of an initial baseline phase with unaltered feedback followed by a training period in which the first formant frequency (f1) of the auditory feedback was shifted downward. Figure 1*A* shows the spectrograms of the target vowel utterance /e/ (as in "Head") with its produced f1 marked in blue and the downward shifted auditory feedback /ɪ/ (sounded as "Hid") marked in red. The response to the altered feedback during the training phase varied across subjects and resulted in two different outcomes: nine subjects who adapted to the task (henceforth "adapters") compensated for the auditory perturbation by gradually shifting the f1 production upwards so that the auditory feedback received at the end of the training matched closely the target vowel sound /ae/, while eight subjects did not adapt to the perturbation (henceforth "nonadapters"). Figure 1*B* shows the produced f1, normalized relative to the baseline and averaged across subjects, for both adapters and nonadapters. In the baseline phase, the formant production is similar for both groups. During the training phase, the f1 production showed upward compensation in response to downward auditory shift is clearly evident for the adapters, whereas for the nonadapters the production seemed to follow the perturbation. A split-plot ANOVA revealed significant differences between the two groups [$F(1, 15) = 6.61$, $P < 0.025$] with a significant interaction ($P < 0.05$). A post hoc analysis revealed significant differences between the two groups at late training at $P < 0.01$. To quantify outcome differences, a straight line was fitted on the training data and its slope was used as a measure of adaptation; a significant positive slope indicates successful compensation to auditory perturbation.

The locations of the EEG recording electrodes are shown in Fig. 1*C*. The signals were aligned at the voice onset and were divided into three epochs for analyses (Fig. 1*D*). A time window of −300 ms to the voice onset (at 0 ms) was defined as the speech-planning epoch; from 0 to 300 ms as the speech-production epoch; from 300 to 600 ms as the postproduction epoch. This partitioning allowed us to study the dynamics of the neural activity at temporal windows before, during, and following each utterance so as to capture planning, production, and feedback error processing related activity during utterances. As the motor training proceeded, we monitored how neural activity changed in these time windows during the feedforward and feedback processes that accompany speech motor adaptation. Thus activity during the planning epoch shed light on motor preparation and feedforward control, while activity during speech production captures motor control, and while the postproduction epoch highlights later stages of feedback error processing and updating of existing motor maps. To capture the evolution of neural activity with training, we took the last 30% of the baseline trials (baseline), the first 30% of the training trials (early training), and the last 30% of the training trials (late training). By focusing on baseline and early and late training, we were able to determine how feedforward and feedback processes evolved over the course training and how they differed between adapters and nonadapters.

To understand the contributions of the various frequency bands toward adaptation, we worked with the instantaneous power of the neural activity within each band. Our first step was to see if and how the power traces of the various EEG frequency band changed with training. Figure 1*D* shows the time series of the total power averaged over across all subjects for each frequency band and at different experimental phases for a representative electrode location CPz during the baseline, early, and late training phases (adapters in blue, nonadapters in red). For this electrode, distinct activation patterns between the two groups emerged at late training suggesting contrasting brain activity accompanying their behavioral differences. Figure 2 further shows scalp plots for the five different EEG frequency bands, delta, theta, alpha, beta, and gamma, that capture mean differences in neural activity between the adapters and the nonadapters. This was obtained for each group by averaging the total power in each band over all the speech epochs (300 ms before the voice onset to 600 ms after) and then taking the difference between the two groups. Even in this large window of averaging, the scalp plots clearly show widespread power differences across all EEG frequency bands between the two groups providing the first indications that EEG band power profiles are likely contain information about differences in speech motor adaptation.

Our next objective was to identify the electrode locations within each frequency band at different training phases that contained information about adaptation outcomes. We first used a GLM to identify the electrode locations whose power

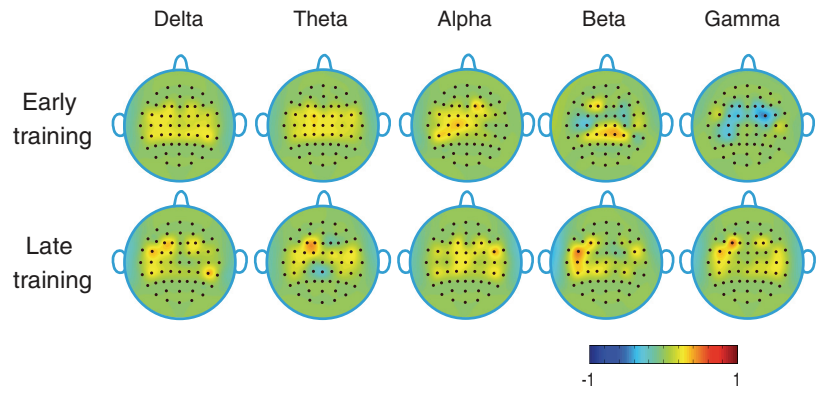

Fig. 2. Power scalp plots. Power differences between adapters and nonadapters are shown at late and early training and for different EEG frequency bands. These are averaged across subjects and over all speech epochs. Power differences are widespread over different scalp regions. Positive values indicate higher power levels for adapters compared with nonadapters and vice versa.

levels carry information about the outcome differences in the speech motor task at $P < 0.01$ (uncorrected). Electrode locations at $P < 0.01$ that are corrected for multiple comparisons are shown by white dots. Figure 3 shows the scalp plot of the electrode locations at early and late training; hotter colors (red) indicate positive correlation between power levels and adaptation outcomes while colder (blue) colors indicate negative correlations. At early training, all frequency bands except the delta band contained information about differences in adaptation outcome. The theta band did not show any power activity that significantly correlated with the adaptation during the planning phase. The information-bearing beta-power level was primarily bilateral while alpha and gamma bands mostly had right lateral activation during the planning phase. Gamma power during speech planning was found to have an inverse relation (blue) between power level and amount of adaptation, i.e., the greater the amount of adaptation, lower the level of gamma activation, and vice versa. During production, the theta-, beta-, and gamma-band power carried information in parietal and frontal electrodes, while during postproduction, the theta and gamma bands were most informative.

By late training however, the behaviorally correlated power activity patterns had changed in almost all the bands but most significantly in the theta, beta, and gamma bands (Fig. 3). The delta band showed localized power differences in the planning phase in the left front-temporal electrodes. The theta-band power changed dramatically; the prominent early training activation seen in the postproduction phase disappeared, and instead we observed bilateral activation during speech-planning and speech-production phases over fronto-temporal electrodes; a slight negative left lateralized theta activation was also seen during postproduction. Alpha-band power change was restricted entirely in the planning phase at the frontal, parietal, and right-temporal electrodes. The beta band showed differences at centro-parietal electrodes during planning and significant bilateral activation during production, while slightly right-lateralized activation during postproduction. The gamma band power activity was the strongest and the most widespread. It spanned all epochs of speech planning, production, and postproduction and covered significant regions over the scalp. During planning strong positive centro-parietal and frontal activity was accompanied by slight negative bilateral activation in the frontal scalp location. During production, the power activation was the strongest and spanned large regions of the parietal and frontal areas of the scalp. Strong activation was also observed in the right parietal scalp region. This was followed by a decrease in power level in the postproduction epoch, although strong positive activation was still seen over the centro-parietal and fronto-parietal scalp region and some limited activation in the right-fronto-temporal regions. It should be noted that theta- and gamma-band activities are strongly implicated during speech planning while the beta band is in the production epoch.

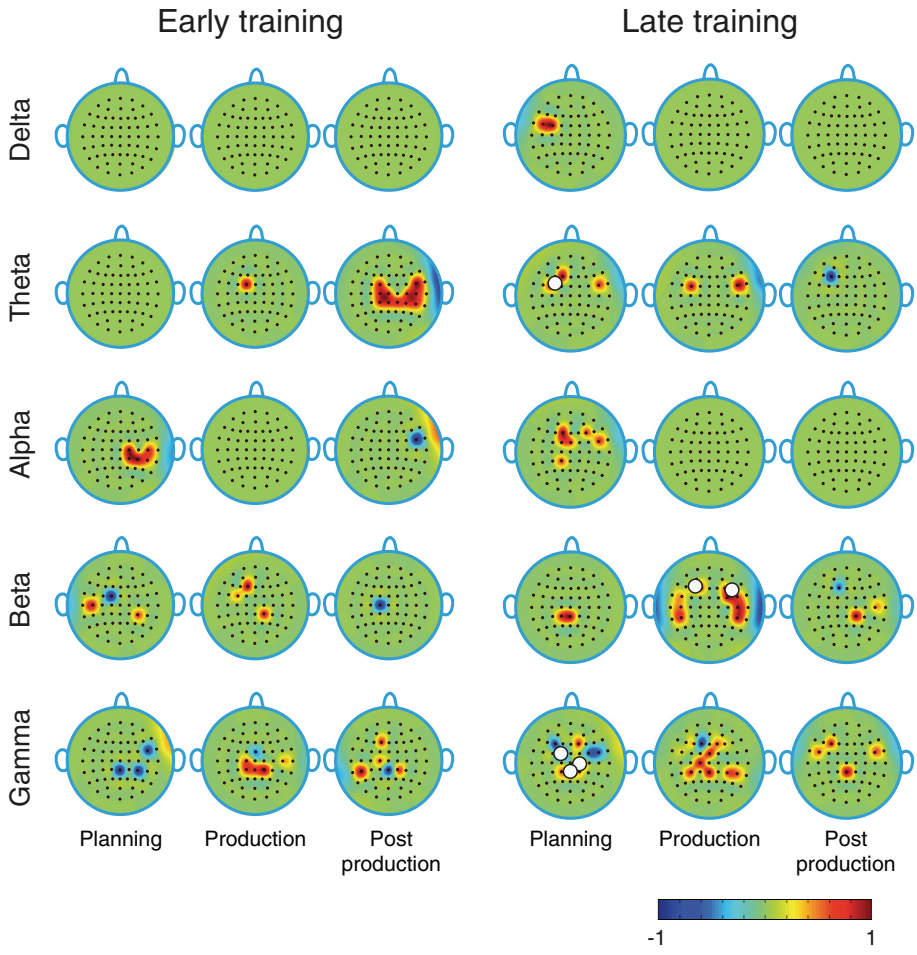

Fig. 3. Generalized linear model (GLM) and electrode locations. The electrode locations carrying information about adaptation were identified using the GLM analyses. Plotted are the GLM coefficients at $P < 0.01$. White dots show electrode locations at $P < 0.01$, corrected for multiple comparisons. Red (hot) colors are for positive coefficients and, blue (cooler) colors are for negative coefficients. At early training, there was no delta band activity while at late training it showed up only during the speech-planning epoch. At early training no theta activity was seen during speech planning while more prominent activity was seen during postproduction. At late training theta band showed fronto-temporal activation during planning and production, with a stronger left lateralization. Alpha-band activity was observed during planning epoch both at early and late training phases. Beta-band activity was observed at early and late training for all the three speech epochs. As with the beta band, gamma band involved wide spread scalp regions for all speech epochs, increasing during speech planning and speech production during late training. Observe the increase in activity in theta, beta, and gamma bands during late training relative to early training, suggesting adaptation related changes.

To further corroborate the above findings, we next examined whether the neural activity that correlated with adaptation according to the GLM model at the identified electrodes could predict the outcome of the speech motor task. To answer this question we performed blind linear classification analyses at early and late training for all three speech epochs (baseline phase did not contain any predictive information). This allowed us to gauge the predictive strength of scalp activity within the different EEG frequency bands in differentiating the adapters from the nonadapters with at least 80% accuracy (see METHODS). Figure 4 shows results from the classification analyses (white dots show the GLM electrode locations at $P < 0.01$ corrected for multiple comparisons). At early training, the scalp power levels at none of the frequency band was predictive of adaptability. By late training, however, the theta-, beta-, and gamma-band power levels were found to reliably differentiate adapters from nonadapters. The theta band only had one electrode location, Fc3 on the left frontal scalp region, the power level of which only during speech-planning could predict outcome differences. In contrast, the beta-band power levels during all three epochs were found to be reliably predicting adaptability. During speech planning, beta activity at the centro-parietal electrode location, Cpz; during speech production, activities at the electrode locations in the fronto-temporal regions, F3 and Fc5; left centro-parietal region, Cp5; and right fronto-central location, Fc6; and during postproduction phase, activities at frontal location, F1; and centro-parietal region, Cp2, were predictive of adaptability. The gamma-band power level showed extensive predictive capacity but was restricted only during the planning and production epochs both of which contained bilateral parietal and the frontal scalp regions. During speech planning, right temporal, frontal, and parietal activation at electrode locations F1, F2, F4, Fc1, Fc4, C2, Cpz, and Cp6 was found to be reliable predictors, while during production, parietal and frontal power levels at F1, F2, and Cpz were found to be reliable predictors of adaptability. Thus GLM and classification analyses together strongly implicate theta, beta, and gamma bands in supporting motor speech adaptability.

It is rather remarkable that high mean classification accuracy of 80% was obtained in a large number (4,000) of bootstrapped samples despite the training and test sets in each bootstrapped samples contained roughly the same number of subjects, which makes the classification task much harder. At the threshold crossings where the mean classification accuracy for the bootstrapped samples exceeds 0.5 (classification at the chance level), the corresponding probability is $P < 10^{-8}$ (see METHODS). To further determine the statistical significance of clas-

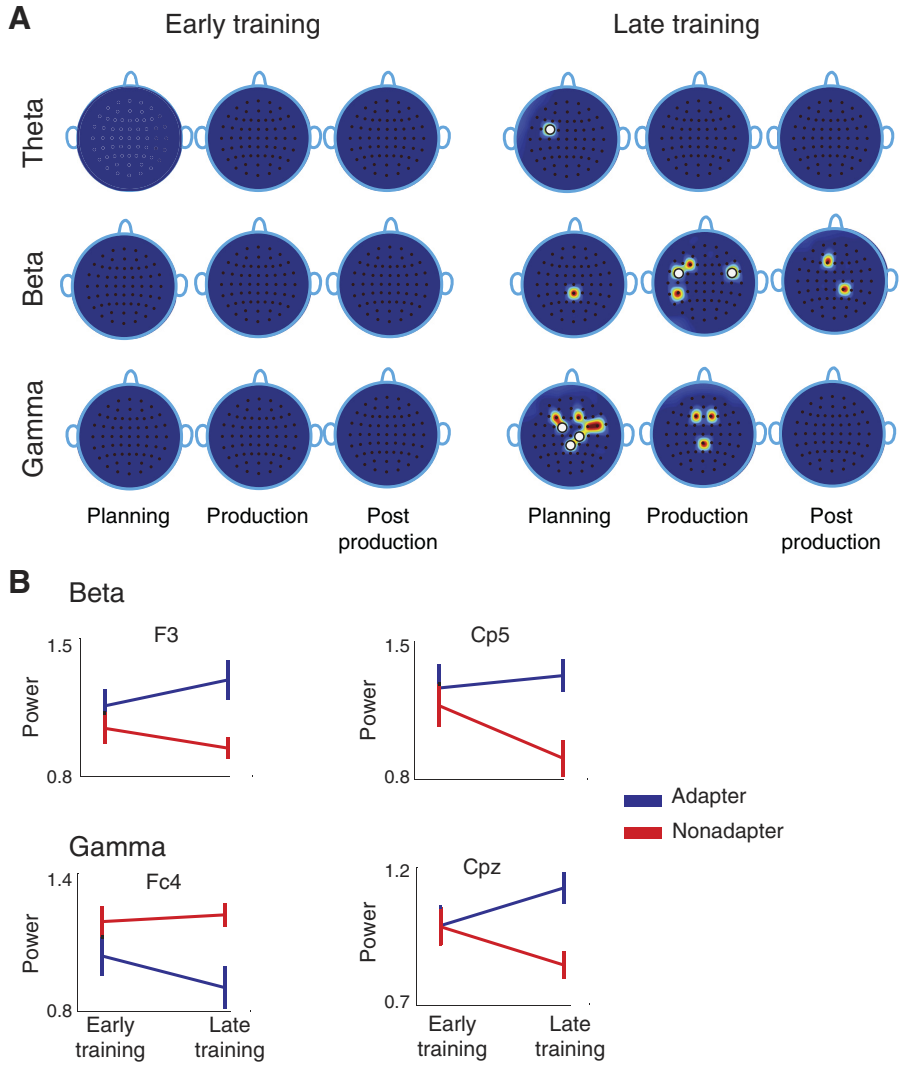

Fig. 4. Motor speech adaptability for different EEG frequency bands. Linear classification was used to assess information contained in different EEG frequency bands about predicting outcome differences in the speech motor task. Only the theta-, beta-, and gamma-band activities at late training were found to be reliable predictors of motor speech adaptability. The significant electrode locations are marked in red. During speech planning and production epochs all three bands were involved, whereas during postproduction only the beta band activity showed up. Left centro-parietal electrode in theta band was seen during planning. In beta band, left parietal electrodes during planning, left parietal area during production and localized right-parietal and left-frontal electrode during late production. Widespread central and parietal activation during planning and localized central and frontal activation during production was seen in gamma. *B*: the power levels at early and late training for two representative electrodes are shown in gamma and beta bands. Note that although the adapters and nonadapters did not differ in their power levels at early training, differences between them emerged by late training. White dots show GLM electrode locations at $P < 0.01$, corrected for multiple comparisons.

sification results, group differences in the power level for each band and at each electrode location were assessed under the *t*-test and separately using a repeated-measures ANOVA. Wherever the classifier crossed the threshold of 80%, there were significant power differences between the adapters and nonadapters under ANOVA (see METHODS) or *t*-test ($P < 0.05$ or less). The theta-band activity for electrode Fc3 showed significance only under the *t*-test at $P < 0.01$. Most of the beta-band electrodes showed significance under the ANOVA followed by a post hoc test: F3, $F(1, 15) = 7.69$, $P < 0.01$; Fc6, $F(1, 15) = 7.51$, $P < 0.01$; Cp5, $F(1, 15) = 6.1$, $P < 0.03$; Cp2, $F(1, 15) = 11.7$, $P < 0.001$ (quoted here and below are only the F values of the main effect showing the group differences). The electrode Fc5 was significant only under the *t*-test at $P < 0.005$. Likewise, most of the gamma-band electrodes showed significance under the ANOVA: F1, $F(1, 15) = 12.08$, $P < 0.001$; Fc1, $F(1, 15) = 5$, $P < 0.03$; Fc4, $F(1, 15) = 9$, $P < 0.01$; C2, $F(1, 15) = 5.6$, $P < 0.02$; Cpz, $F(1, 15) = 5.6$, $P < 0.02$. The remaining electrodes were significant under the *t*-test: F2: $P < 0.005$; Fc1: < 0.02. Figure 4*B* shows power levels for two representative electrodes from beta and gamma band at early and late training. It can clearly be seen that power differences between the adapters and nonadapters emerge by late training. It should be noted that the ANOVA and *t*-tests were conducted in the same temporal window in which the classification results were obtained, suggesting that although the classification analyses and ANOVA tap into different types of information, there was a close agreement between the two methods.

The classification analyses thus established that theta, gamma, and beta bands not only contained information about speech motor adaptation and that these activities were reliable predictors of outcome differences in speech motor adaptation, while delta and alpha bands did not contain any reliable information in any of the epochs on which such a classification could be made. It was thus natural to ask if the bands operated independently or if they were coupled to each other to mediate adaptation and whether such coupling could potentially arise from common underlying sources. We found very little overlap in the electrodes across the different frequency bands. To address this issue, PC analyses were performed to estimate the EEG sources that could be contributing to the scalp activity. We extracted the first three PCs associated with each EEG frequency band that accounted for at least 80% of the variance in the data. The power time series of these PCs are shown in Fig. 5*A* (adapters in blue, nonadapters in red). Observe the distinct activities between the two groups emerging by late training. We ran classification analyses on each PC and for each frequency band and found that, at late training, only the third PC (PC3) of the theta band, the second of the beta band (PC2), and the third of the gamma band (PC3) were reliable predictors of adaptability (Fig. 5*B*), while delta and alpha bands did not clear the cutoff in any of the PC components. This was consistent with the results obtained at the scalp level in which the theta, beta, and gamma activities at late training were also found to be the only reliable predictors.

Finally, we proceeded to quantify the interband interaction by carrying out covariance analysis between PCs (Fig. 5*C*) that is similar to computing spectral coherence. Significant interactions were found across the PCs of theta-, beta-, and gamma-band pairs that crossed the classification threshold. Notably, at late training there was a prominent interaction between a PC in the theta band and a PC in the gamma band ($P < 0.0005$, uncorrected). Note that theta-gamma interaction in terms of neural phase coherence was previously observed for adapters (Sengupta and Nasir 2015). Adapters showed stronger positive covariance while nonadapters showed a negative covariance resulting in a mean covariance difference of 0.44 between the two groups. Interaction to a lesser extent was also seen at late training between the beta and the gamma bands ($P <$

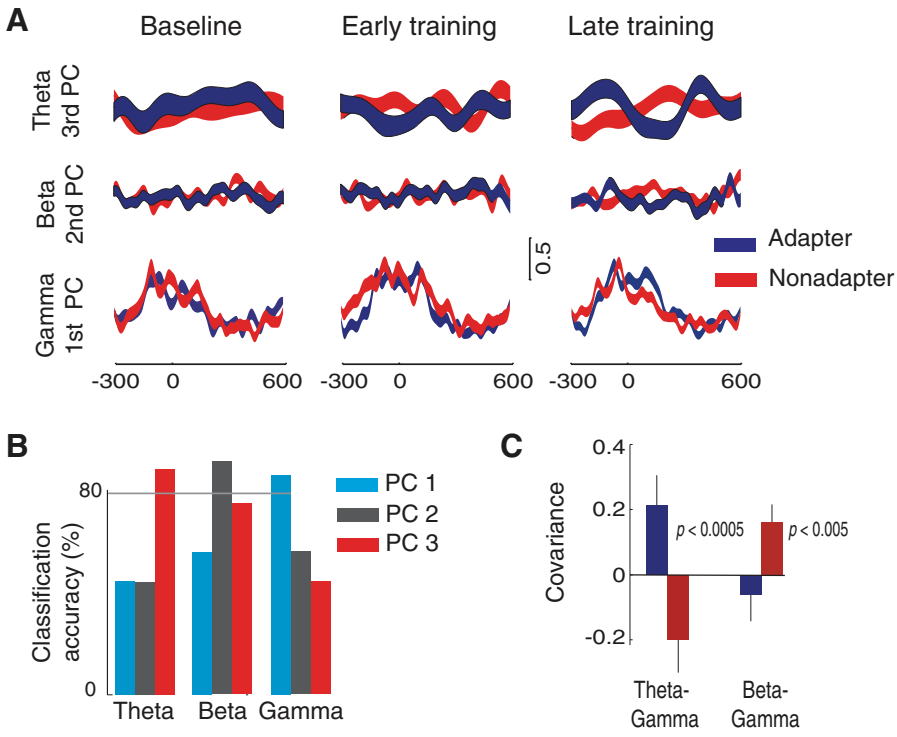

Fig. 5. Estimating interband interaction. *A*: principal components were computed to estimate neural sources and quantify interaction across the bands. At late training only the third principal component of the theta band, the second of the beta band and the third of the gamma band were reliable predictors of adaptability. These principal component traces averaged across adapters (blue) and nonadapters (red) are shown for different experimental phases. Note the differences arising during early training, becoming more amplified by late training phase. *B*: shown are classification accuracy for the principal components. *C*: interband interaction was estimated by computing the covariance between power bands and comparing between adapters and nonadapters. Significant interaction was seen between theta and gamma band and also between gamma and beta bands.

0.005, uncorrected) with a resulting mean difference of −0.15 between the two groups. Thus the gamma bands interact with both theta and beta bands and the theta- and gamma-band interaction appears to facilitate adaptation while beta- and gamma-band interaction inhibiting adaptation.

DISCUSSION

We have studied speech motor adaptation under altered auditory feedback with the goal of identifying the neural signatures that underlie motor speech adaptability. We argued that by identifying the neural processes that robustly distinguish adapters from nonadapters, we could unravel the neural signatures of speech motor adaptation. In particular, identification of frequency bands and the temporal window of their activation within speech utterances that contain behaviorally relevant information and whose activities predict the outcome of speech motor adaptation reveals a dynamic picture of specific oscillatory processes and their contributions towards adaptation can be obtained. We proceeded to first identify the set of electrodes whose power activity correlated with behavior using a GLM and then, using a linear classifier, assessed their predictive accuracy to obtain a smaller set of electrodes that was highly informative of the behavioral outcome. These analyses were carried out at different epochs of speech utterance to identify electrodes and frequency bands that contributed to speech planning and production. It was found that by late training, the instantaneous power in theta and gamma bands during speech planning and beta band during speech production contained predictive information about adaptation outcomes. While theta-band power was localized to fronto-temporal electrodes, gamma-band activity was more widespread spanning temporal and parietal electrodes on the scalp and beta-band activity was restricted mostly to temporal electrodes. Finally, to understand to what extent scalp power activations reflect interaction between the frequency bands at the level of underlying sources we performed PC analyses that revealed high degree of interaction between the bands. Since low-frequency bands are believed to reflect synchronized distributed activities while high-frequency bands more localized activity (Von Stein and Sarnthein 2000), these correlations across the frequency bands suggest a larger underlying network operating across multiple frequency bands in hierarchical fashion.

The GLM analyses revealed a subset of electrodes in all the EEG frequency bands being implicated in speech motor adaptation, but not all of them were predictive of adaptation outcomes. This is likely due to the reason that although numerous processes involved in mediating speech motor adaptation are distributed across multiple brain areas, all of them may not be directly involved in the recalibration of the motor maps necessary for successful adaptation. It is also interesting to note that it was only by late training when the theta, beta, and gamma bands contained enough predictive information to successfully classify adapters from nonadapters. These results are in good agreement with prior studies that have shown the involvement of theta and gamma bands in motor adaptation (Perfetti et. al 2011; Sengupta and Nasir 2015) and the role of the beta band in anticipating sensory events during motor planning (Arnal and Giraud 2012). The theta, beta, and gamma powers during speech planning were found to be predictive of motor speech adaptability suggesting a more direct role played by these bands in the establishment of a new feedforward map associated with adaptation; in contrast, the alpha and delta bands play little role in the process. The beta and gamma bands were implicated during speech production suggesting a role for them in feedback error monitoring. During the postproduction epoch, only beta band activity was predictive of adaptability that suggests the involvement of beta band in a late stage feedback processing. It should also be noted theta and beta bands showed a more limited scalp activity than the gamma band whose activity was more widespread.

As multiple scalp activity patterns could result from a single underlying source (Michel et. al. 1992), we speculated that a small number of oscillatory neural mechanisms involved in accounting for differences in motor speech adaptability, possibly neural sources located beneath the left-temporal and centro-parietal scalp regions that support the feedback and feedforward processes, respectively. The PC analyses revealed that only the first few components for the theta, beta, and gamma bands contained predictive information about adaptation outcomes, which further points to a handful of underlying oscillatory processes that may be driving these changes. Under the assumption that activities at different EEG frequency bands reflect brain networks at different scales (Siegel et al. 2012; Hipp et al. 2011, 2012; Von Stein and Sarnthein 2000; Bullmore and Sporns 2009), one could ask how these networks interact in mediating motor speech adaptability. The covariance analyses revealed pairwise interactions between the theta and gamma and between the beta and the gamma bands. It is very possible that this interaction could result from coupling factors such as cross-frequency phase coherence between beta and theta bands and between gamma and theta bands, which have been shown to play a critical role in motor adaptation and learning in a variety of behaviors including speech (Sengupta and Nasir 2015; Perfetti et. al. 2011). Overall, the pairwise interactions across the bands imply interactions between a smaller and local network (gamma activity) and networks at medium and large scale (beta and theta bands).

What are the neural sources and the brain networks that generate the observed power differences in the theta, beta, and gamma bands? A series of functional (f)MRI studies by Guenther and his colleagues identified brain areas in premotor cortex and superior temporal cortex for the processing of auditory feedback error (Tourville et al. 2008). Learning of novel speech motor sequence involved pre-supplementary motor area (Segawa et al. 2014). According to the DIVA model the feedforward part of the speech motor system consists of the supplementary motor area, basal ganglia, premotor, and motor cortex; the feedback processing system contains ventral premotor cortex, planum temporale, and posterior superior temporal gyrus (Golfinopoulos et. al. 2010). It remains to be seen if the same brain areas are also implicated in the EEG frequency bands underlying motor speech adaptation. The theta band, for example, is found to encompass a fronto-parietal network in a visual task (von Stein and Sarnthein 2000) or the medial temporal lobe in case of spontaneous cortical activity (Hipp et al. 2012). Likewise, the beta band involves parietal areas and the gamma band describes local neuronal processing and may involve pareito-temporal or sensorimotor areas (von Stein and Sarnthein 2000; Hipp et al. 2011, 2012). To find the proper correspondence between the EEG and fMRI results, a

detailed source reconstruction analysis needs to be conducted. Infact, the same feedback alteration paradigm in conjunction with simultaneous recording of EEG and fMRI could be conducted to investigate such correspondences.

To the best of our knowledge, this is the first study demonstrating the predictive capacity of neural oscillations in determining behavioral outcome in speech motor adaptation. An application of this predictive method is well suited for clinical application for the understanding of speech disorders (Gonzalez-Gadea et al. 2015; Markser et al. 2015; Kamavuako et al. 2015; Dickinson et al. 2015). By comparing brain activity between healthy and disordered population at relevant electrode locations and frequency bands, it may be possible to isolate processes that are most informative about an underlying disorder. Since our method developed here may expose differences and anomalies during both speech perception and production, it has the potential to shed light on more specific sensory and motor processes that break down in the speech chain in disorders. Neural oscillations, in particular, may be used to probe into anomalous patterns in neural communications within and across the various brain regions that may underlie speech disorders such as stuttering and aphasia. Identifying the specific locus and time course of anomalous activity will yield greater insight into the specific causes of speech disorders and thus help clinicians in devising more effective treatment suited to individual patient needs. The methods presented may therefore be applicable to novel noninvasive EEG-based diagnostic methods in motor speech disorders.

An important question that arises from this and past studies is regarding the nature of the roles that the various frequency bands play in sensorimotor learning. Why are theta, gamma, and beta bands important in motor speech, and not the others? What specific functional roles do they serve? To answer this question, we must look into developmental trajectories of the various frequency bands. Whether same bands also important in children learning to speak and can predict their degree of speech learning will further help to elucidate the roles of the individual bands and their interactions. Developmental studies such as this, along with closer inspection of disordered populations, will bring further clarity into the exact nature of the various frequency bands in speech motor learning and adaptation.

DISCLOSURES

No conflicts of interest, financial or otherwise, are declared by the author(s).

AUTHOR CONTRIBUTIONS

R.S. and S.M.N. conception and design of research; R.S. performed experiments; R.S. analyzed data; R.S. and S.M.N. interpreted results of experiments; R.S. prepared figures; R.S. drafted manuscript; R.S. and S.M.N. edited and revised manuscript; R.S. and S.M.N. approved final version of manuscript.

REFERENCES

Arnal LH, Giraud AL. Cortical oscillations and sensory predictions. *Trends Cogn Sci* 16: 390–398, 2012.

Arnal LH, Wyart V, Giraud AL. Transitions in neural oscillations reflect prediction errors generated in audiovisual speech. *Nat Neurosci* 14: 797–801, 2011.

Brodski A, Paasch GF, Helbling S, Wibral M. The faces of predictive coding. *J Neurosci* 35: 8997–9006, 2015.

Bullmore E, Sporns O. Complex brain networks: graph theoretical analysis of structural and functional systems. *Nat Rev Neurosci* 10: 186–198, 2009.

Cai S, Beal DS, Ghosh SS, Tiede MK, Guenther FH, Perkell JS. Weak responses to auditory feedback perturbation during articulation in persons who stutter: evidence for abnormal auditory-motor transformation. *PLoS One* 7: e41830, 2012.

Canolty RT, Edwards E, Dalal SS, Soltani M, Nagarajan SS, Kirsch HE, Berger MS, Barbaro NM, Knight RT. High gamma power is phase-locked to theta oscillations in human neocortex. *Science* 313: 1626–1628, 2006.

Cheyne D, Bells S, Ferrari P, Gaetz W, Bostan AC. Self-paced movements induce high-frequency gamma oscillations in primary motor cortex. *Neuroimage* 42: 3323–3342, 2008.

Douglas C, Bells S, Ferrari P, Gaetz W, Bostan AC. Self-paced movements induce high-frequency gamma oscillations in primary motor cortex. *Neuroimage* 42: 332–342, 2008.

Dickinson A, Bruyns-Haylett M, Jones M, Milne E. Increased peak gamma frequency in individuals with higher levels of autistic traits. *Eur J Neurosci* 8: 1095–1101, 2015.

Efron B. *The Jackknife, the Bootstrap, and Other Resampling Plans*. Philadelphia, PA: SIAM, 1982.

Freyer F, Becker R, Dinse HR, Ritter P. State-dependent perceptual learning. *J Neurosci* 33: 2900–2907, 2013.

Friedman JH, Tibshirani R, Hastie T. *The Elements of Statistical Learning* (2nd ed.). New York: Springer, 2009.

Giraud AL, Poeppel D. Cortical oscillations and speech processing: emerging computational principles and operations. *Nat Neurosci* 15: 511–517, 2012.

Golfinopoulos E, Tourville JA, Guenther FH. The integration of large-scale neural network modeling and functional brain imaging in speech motor control. *Neuroimage* 52: 862–874, 2010.

Gonzalez-Gadea ML, Chennu S, Bekinschtein TA, Rattazzi A, Beraudi A, Trippichio P, Moyano B, Soffita Y, Steinberg L, Adolfi F, Sigman M, Marino J, Manes F, Ibanez A. Predictive coding in autism spectrum disorder and attention deficit hyperactivity disorder. *J Neurophysiol* 114: 2625–2636, 2015.

Guenther FH. Cortical interactions underlying the production of speech sounds. *J Commun Disord* 39: 350–365, 2006.

Hipp JF, Hawellek DJ, Corbetta M, Siegel M, Engel AK. Large-scale cortical correlation structure of spontaneous oscillatory activity. *Nat Neurosci* 15: 884–890, 2012.

Hipp JF, Engel AK, Siegel M. Oscillatory synchronization in large-scale cortical networks predicts perception. *Neuron* 69: 387–396, 2011.

Houde JF, Jordan MI. Sensorimotor adaptation in speech production. *Science* 279: 1213–1216, 1998.

Jones JA, Munhall KG. Remapping auditory-motor representations in voice production. *Curr Biol* 15: 1768–1772, 2005.

Kamavuako EN, Jochumsen M, Niazi IK, Dremstrup K. Comparison of features for movement prediction from single-trial movement-related cortical potentials in healthy subjects and stroke patients. *Comput Intell Neurosci* 2015: 858015, 2015.

Lametti DR, Nasir SM, Ostry DJ. Sensory preference in speech production revealed by simultaneous alteration of auditory and somatosensory feedback. *J Neurosci* 32: 9351–9358, 2012.

Lisman JE, Jensen O. The theta-gamma neural code. *Neuron* 77: 1002–1016, 2013.

Markser A, Maier F, Lewis CJ, Dembek TA, Pedrosa D, Eggers C, Timmermann L, Kalbe E, Fink GR, Burghaus L. Deep brain stimulation and cognitive decline in Parkinson's disease: the predictive value of electroencephalography. *J Neurol* 262: 2275–2284, 2015.

McCullagh P, Nelder J. *Generalized Linear Models* (2nd ed.). Boca Raton, FL: Chapman and Hall/CRC, 1989.

McFarland DJ, Miner LA, Vaughan TM, Wolpaw JR. Mu and beta rhythm topographies during motor imagery and actual movements. *Brain Topogr* 12: 177–186, 2000.

Michel CM, Lehmann D, Henggeler B, Brandeis D. Localization of the sources of EEG delta, theta, alpha and beta frequency bands using the FFT dipole approximation. *Electroencephalogr Clin Neurophysiol* 82: 38–44, 1992.

Myers NE, Stokes MG, Walther L, Nobre AC. Oscillatory brain state predicts variability in working memory. *J Neurosci* 34: 7735–7743, 2014.

Nasir SM, Ostry DJ. Somatosensory precision in speech production. *Curr Biol* 16: 1918–1923, 2006.

Olbrich S, Jödicke J, Sander C, Himmerich H, Hegerl U. ICA-based muscle artefact correction of EEG data: what is muscle and what is brain? *Neuroimage* 54: 1–3, 2011.

Perfetti BP, Moisello C, Landsness EC, Kvint S, Lanzafame S, Onofrj M, Di Rocco A, Tononi G, Ghilardi MF. Modulation of gamma and theta spectral amplitude and phase synchronization is associated with the development of visuo-motor learning. *J Neurosci* 31: 14810–14819, 2011.

Perkell J. Movement goals and feedback and feedforward control mechanisms in speech production. *J Neurolinguistics* 25: 382–407, 2012.

Purcell DW, Munhall KG. Adaptive control of vowel formant frequency: evidence from real-time formant manipulation. *J Acoust Soc Am* 120: 966–977, 2006.

Quandt F, Reichert C, Hinrichs H, Heinze HJ, Knight RT, Rieger JW. Single trial discrimination of individual finger movements on one hand: a combined MEG and EEG study. *Neuroimage* 59: 3316–3324, 2012.

Segawa JA, Tourville JA, Beal DS, Guenther FH. The neural correlates of speech motor sequence learning. *J Cogn Neurosci* 27: 819–831, 2014.

Sengupta R, Nasir SM. Redistribution of neural phase coherence reflects establishment of feedforward map in speech motor adaptation. *J Neurophysiol* 113: 2471–2479, 2015.

Siegel M, Donner TH, Engel AK. Spectral fingerprints of large-scale neuronal interactions. *Nat Rev Neurosci* 13: 121–134, 2012.

Strauss A, Kotz SA, Scharinger M, Obleser J. Alpha and theta brain oscillations index dissociable processes in spoken word recognition. *Neuroimage* 97: 387–395, 2014.

Tourville JA, Reilly KJ, Guenther FH. Neural mechanisms underlying auditory feedback control of speech. *Neuroimage* 39: 1429–1443, 2008.

Tremblay S, Shiller DM, Ostry DJ. Somatosensory basis of speech production. *Nature* 423: 866–869, 2003.

Tzagarakis C, Ince NF, Leuthold AC, Pellizzer G. Beta-band activity during motor planning reflects response uncertainty. *J Neurosci* 30: 11270–11277, 2010.

van Wijk BC, Beek PJ, Daffertshofer A. Neural synchrony within the motor system: what have we learned so far? *Front Hum Neurosci* 6: 252, 2012.

Villacorta VM, Perkell JS, Guenther FH. Sensorimotor adaptation to feedback perturbations of vowel acoustics and its relation to perception. *J Acoust Soc Am* 122: 2306–2319, 2007.

von Stein A, Sarnthein J. Different frequencies for different scales of cortical integration: from local gamma to long range alpha/theta synchronization. *Int J Psychophysiol* 38: 301–313, 2000.

Waldert S, Preissl H, Demandt E, Braun C, Birbaumer N, Aertsen A, Mehring C. Hand movement direction decoded from MEG and EEG. *J Neurosci* 28: 1000–1008, 2008.

Wang W, Sudre GP, Xu Y, Kass RE, Collinger JL, Degenhart AD, Bagic AI, Weber DJ. Decoding and cortical source localization for intended movement direction with MEG. *J Neurophysiol* 104: 2451–2461, 2010.

Ziegler W, Wessel K. Speech timing in ataxic disorders Sentence production and rapid repetitive articulation. *Neurology* 47: 208–214, 1996.